Chemistry of Hydrogen Oxide Radicals \((HO_x)\) in the Arctic Troposphere in Spring

Atmos. Chem. Phys., 10, 5823–5838, 2010
www.atmos-chem-phys.net/10/5823/2010/
doi:10.5194/acp-10-5823-2010

Atmospheric Chemistry and Physics

Chemistry of hydrogen oxide radicals (HO_x) in the Arctic troposphere in spring

J. Mao[1], D. J. Jacob[1,2], M. J. Evans[3], J. R. Olson[4], X. Ren[5], W. H. Brune[6], J. M. St. Clair[7], J. D. Crounse[7], K. M. Spencer[7], M. R. Beaver[7], P. O. Wennberg[8,9], M. J. Cubison[10], J. L. Jimenez[10], A. Fried[11], P. Weibring[11], J. G. Walega[11], S. R. Hall[12], A. J. Weinheimer[12], R. C. Cohen[13], G. Chen[4], J. H. Crawford[4], C. McNaughton[14], A. D. Clarke[14], L. Jaeglé[15], J. A. Fisher[2], R. M. Yantosca[1], P. Le Sager[1,*], and C. Carouge[1]

[1]School of Engineering and Applied Sciences, Harvard University, Cambridge, MA, USA
[2]Department of Earth and Planetary Sciences, Harvard University, Cambridge, MA, USA
[3]School of Earth and the Environment, University of Leeds, Leeds, LS2 9JT, UK
[4]Science Directorate, NASA Langley Research Center, Hampton, VA, USA
[5]Rosenstiel School of Marine and Atmospheric Science, University of Miami, Miami, FL, USA
[6]Department of Meteorology, Pennsylvania State University, University Park, PA, USA
[7]Division of Chemistry and Chemical Engineering, California Institute of Technology, Pasadena, CA, USA
[8]Division of Geological and Planetary Sciences, California Institute of Technology, Pasadena, CA, USA
[9]Division of Engineering and Applied Science, California Institute of Technology, Pasadena, CA, USA
[10]Department of Chemistry and Biochemistry and Cooperative Institute for Research in the Environmental Sciences (CIRES),University of Colorado at Boulder, Boulder, CO, USA
[11]Earth Observing Laboratory, National Center for Atmospheric Research, Boulder, CO, USA
[12]Atmospheric Chemistry Division, National Center for Atmospheric Research, Boulder, CO, USA
[13]Department of Chemistry and Department of Earth and Planetary Science, University of California Berkeley, Berkeley, CA, USA
[14]University of Hawaii at Manoa, Honolulu, Hawaii, USA
[15]Department of Atmospheric Sciences, University of Washington, Seattle, Washington, USA
[*]now at: KNMI, Chemistry and Climate Division, De Bilt, The Netherlands

Received: 3 March 2010 – Published in Atmos. Chem. Phys. Discuss.: 11 March 2010
Revised: 13 June 2010 – Accepted: 21 June 2010 – Published: 1 July 2010

Abstract. We use observations from the April 2008 NASA ARCTAS aircraft campaign to the North American Arctic, interpreted with a global 3-D chemical transport model (GEOS-Chem), to better understand the sources and cycling of hydrogen oxide radicals (HO_x≡H+OH+peroxy radicals) and their reservoirs (HO_y≡HO_x+peroxides) in the springtime Arctic atmosphere. We find that a standard gas-phase chemical mechanism overestimates the observed HO_2 and H_2O_2 concentrations. Computation of HO_x and HO_y gas-phase chemical budgets on the basis of the aircraft observations also indicates a large missing sink for both. We hypothesize that this could reflect HO_2 uptake by aerosols, favored by low temperatures and relatively high aerosol loadings, through a mechanism that does not produce H_2O_2. We implemented such an uptake of HO_2 by aerosol in the model using a standard reactive uptake coefficient parameterization with $\gamma(HO_2)$ values ranging from 0.02 at 275 K to 0.5 at 220 K. This successfully reproduces the concentrations and vertical distributions of the different HO_x species and HO_y reservoirs. HO_2 uptake by aerosol is then a major HO_x and HO_y sink, decreasing mean OH and HO_2 concentrations in the Arctic troposphere by 32% and 31% respectively. Better rate and product data for HO_2 uptake by aerosol are needed to understand this role of aerosols in limiting the oxidizing power of the Arctic atmosphere.

Correspondence to: J. Mao
(mao@fas.harvard.edu)

Published by Copernicus Publications on behalf of the European Geosciences Union.

1 Introduction

Radiative forcing by aerosol and tropospheric ozone pollution transported from mid-latitudes may be an important driver of recent Arctic warming (Quinn et al., 2008; Shindell et al., 2008). This pollution is strongest in spring (Scheuer et al., 2003) and is modulated by chemical reactions serving as sources or sinks of aerosols and ozone. The Arctic photochemical environment in spring is characterized by polar sunrise, low sun angles, intense cold, and underlying ice surface. Considerable attention has focused on halogen radical photochemistry under these conditions as a rapid sink for ozone (Simpson et al., 2007), but this appears to be important only in the shallow boundary layer where sea ice provides a halogen radical source (Wagner et al., 2001). Hydrogen oxide radicals ($HO_x \equiv$H+OH+peroxy radicals) have a more pervasive effect in the tropospheric column but the chemistry of these radicals in the Arctic spring has received little study. The OH radical is the principal atmospheric oxidant, affecting both aerosols and ozone in complex ways. Peroxy radical reactions with nitric oxide (NO) are the main chemical source of tropospheric ozone. We use here observations from the April 2008 NASA Arctic Research of the Composition of the Troposphere from Aircraft and Satellites (ARCTAS) aircraft campaign (Jacob et al., 2010), interpreted with a global 3-D chemical transport model (GEOS-Chem CTM), to better understand the sources and cycling of HO_x radicals in the springtime Arctic atmosphere.

HO_x radicals originate from water vapor. The main pathway involves oxidation by the high-energy $O(^1D)$ atom produced from photolysis of ozone:

$$O_3 + h\nu \rightarrow O(^1D) + O_2 \quad \text{(R1)}$$

$$O(^1D) + H_2O \rightarrow 2OH \quad \text{(R2)}$$

The OH atoms cycle with peroxy radicals, driving various HO_x-catalyzed mechanisms for atmospheric oxidation and ozone formation and loss. Oxidation of methane and other volatile organic compounds (VOCs) yields formaldehyde (HCHO), which photolyzes to produce additional HO_x radicals and amplify the original source:

$$HCHO + h\nu \rightarrow H + HCO \quad \text{(R3)}$$

$$H + O_2 + M \rightarrow HO_2 + M \quad \text{(R4)}$$

$$HCO + O_2 \rightarrow HO_2 + CO \quad \text{(R5)}$$

Loss of HO_x eventually takes place by radical-radical reactions. The OH+HO_2 reaction produces water vapor in which case the loss is terminal, but the peroxy+peroxy reactions produce reservoir species such as hydrogen peroxide (H_2O_2) and methyl hydrogen peroxide (CH_3OOH). The peroxides can photolyze to return HO_x radicals. Alternatively, they can be converted to water by reacting with OH or deposited resulting in a terminal HO_x sink. It is useful to define an expanded hydrogen oxides family $HO_y \equiv HO_x$+reservoirs (Jaeglé et al., 2001), where the reservoirs include mainly peroxides but also some other minor reservoir species such as nitrous acid (HONO). The HO_x budget can then be understood on the basis of the HO_y budget and the chemical cycling within the HO_y family, governed in part by reactions involving nitrogen oxide radicals ($NO_x \equiv$NO+NO_2) (Jaeglé et al., 2001). The lifetime of HO_y against conversion to water vapor by reaction of OH with HO_2 or peroxides is of the order of a few days, so that transport of HO_y reservoir species on convective and synoptic scales can modulate the supply of HO_x radicals (Jaeglé et al., 1997; Prather and Jacob, 1997; Müller and Brasseur, 1999).

Past studies of HO_x chemistry in Arctic spring have mainly been from surface sites. They have pointed out the importance of HO_x radical production from photochemically driven snow emissions of H_2O_2 (Hutterli et al., 2001; Jacobi et al., 2002), HCHO (Sumner and Shepson, 1999; Sumner et al., 2002), and HONO (Zhou et al., 2001). They have identified a large photochemical emission of NO_x from snow (Honrath et al., 1999; Ridley et al., 2000) that plays an important role in HO_x cycling (Yang et al., 2002; Chen et al., 2004). Another unique aspect of HO_x chemistry in the boundary layer is the interaction with halogen radicals. These interactions include HO_x production from Br+HCHO (Evans et al., 2003), additional HO_y reservoirs such as HOBr (Bloss et al., 2005), and additional processes for cycling between HO_2 and OH (Simpson et al., 2007).

The Arctic boundary layer is very shallow ($\sim$100 m) and capped by a strong thermal inversion (Kahl, 1990). The atmosphere above is more relevant for the impacts of HO_x chemistry on the Arctic troposphere. It had received little exploration prior to ARCTAS, due to the requirement of an aircraft with comprehensive chemical payload. The Tropospheric Ozone Production about the Spring Equinox (TOPSE) aircraft campaign conducted a series of flights in the North American Arctic from February to May of 2000 including measurements of total peroxy radicals (Cantrell et al., 2003a), HCHO (Fried et al., 2003), and peroxides (Snow et al., 2003) up to 8 km altitude. Photochemical model calculations constrained with these data found (R1) and (R3) to be the major HO_x sources (Wang et al., 2003). However, the model greatly overestimated the observed concentrations of peroxy radicals and H_2O_2 (Cantrell et al., 2003b; Wang et al., 2003) while underestimating HCHO (Fried et al., 2003).

Observations from the ARCTAS aircraft expand greatly on TOPSE in terms of both coverage and chemical payload. ARCTAS vertical profiles extend from the boundary layer to the stratosphere. The payload included measurements of HO_x radicals by two independent methods to resolve experimental uncertainty (Chen et al., 2010). It also included an extensive suite of HO_x precursors, reservoirs, and related species. As we will see, this ensemble of observations offers strong constraints and a new perspective on the factors controlling HO_x concentrations in the Arctic spring troposphere.

2 Data and model

2.1 The ARCTAS campaign

The ARCTAS spring campaign took place from 1 to 21 April, 2008 (Jacob et al., 2010). It included a DC-8 aircraft with a detailed chemical and aerosol payload and a P-3 aircraft with a detailed aerosol and radiation payload. Both were based in Fairbanks, Alaska (65° N, 148° W). We focus our attention on the DC-8 chemical data but will also make reference to the P-3 aerosol data. The DC-8 conducted nine flights in the North American Arctic totaling 73 flight hours. These included sorties out of Fairbanks as well as transit flights to and from Thule, Greenland (77° N, 69° W) and Iqaluit, Nunavut (64° N, 69° W). Almost all the data were collected north of 60° N. All flights included frequent vertical profiling from 100 m to 12 km altitude.

One of the major goals of ARCTAS was to better understand radical photochemistry in the Arctic. The DC-8 payload included measurements of HO_x radicals, NO_x radicals, H_2O_2, CH_3OOH, HNO_4, O_3, H_2O, VOCs, HCHO, aerosol composition, and photolysis frequencies (Jacob et al., 2010). OH and HO_2 concentrations were measured by two independent techniques, Laser Induced Fluorescence (LIF) and Chemical Ionization Mass Spectrometry (CIMS). There were instrumental difficulties with the CIMS HO_2 measurement but intercomparison for OH shows a median ratio $[OH]_{CIMS}/[OH]_{LIF}$=0.73 (R=0.51), which agrees within the stated accuracies (32% for LIF, 65% for CIMS) (Chen et al., 2010). We rely on the LIF measurements here as they covered 96% of the flight hours. We use 1-min average data with reported accuracies in parentheses: OH (32%), HO_2 (32%), H_2O_2 ($\pm$(40%+100 pptv)), CH_3OOH ($\pm$ (76%+50 pptv)), ozone (3%), HCHO (12%$\pm$26 pptv), NO (10%$\pm$5 pptv), NO_2 (5%$\pm$5 pptv), HNO_4 (30%$\pm$15 pptv). We also make use of fine aerosol data including sulfate (34%) and ammonium (34%). The NO_2 LIF measurement includes methylperoxynitrate (CH_3OONO_2) decomposing in the inlet and this represents a significant positive artifact in the upper troposphere (Browne et al., 2010). We correct for it here by using local CH_3OONO_2/NO_2 ratios from the GEOS-Chem simulation. Mean ratios are 0.03 at 0–3 km, 0.17 at 3–6 km, and 1.4 above 6 km.

Several halogen-catalyzed ozone and mercury depletion events were observed during ARCTAS (Salawitch et al., 2010), but all were confined below 500 m. No obvious signature of either bromine or chlorine radical chemistry was found above 500 m from the measured soluble bromide (Liao et al., 2010), BrO (Neuman et al., 2010) or VOC indicators (Fried et al., 2010). We neglect the effect of halogen chemistry in our modeling of the ARCTAS HO_x data but will comment on its possible role in the boundary layer.

2.2 GEOS-Chem model

GEOS-Chem is a global 3-D chemical transport model driven by assimilated meteorological observations from the Goddard Earth Observing System (GEOS-5) of the NASA Global Modeling and Assimilation Office (GMAO) (Bey et al., 2001). We apply here GEOS-Chem version 8-01-04 (http://acmg.seas.harvard.edu/geos/index.html) to simulation of the ARCTAS period (April 2008). The GEOS-5 meteorological data have 6-h temporal resolution (3-h for surface variables and mixing depths) with 0.5°×0.667° horizontal resolution and 72 vertical layers from the surface to 0.01 hPa. We regrid here the meteorological data to 2° latitude × 2.5° longitude for input to GEOS-Chem. The model is initialized with a 1-year simulation from January 2007 to January 2008 with 4°×5° resolution, and from January 2008 on with 2°×2.5° resolution. Our analysis of the GEOS-Chem simulation focuses on HO_x chemistry. The same GEOS-Chem simulation is applied in companion papers to interpretation of ARCTAS observations for CO (Fisher et al., 2010a), sulfate (Fisher et al., 2010b), and carbonaceous aerosols (Wang et al., 2010). The latter two studies show that the model reproduces well the observed aerosol concentrations, lending some confidence in the computation of scavenging and heterogeneous uptake.

We use the standard GEOS-Chem simulation of ozone-NO_x-HO_x-VOC-aerosol chemistry as described for example by Park et al. (2006). We updated the chemical mechanism with compiled data from the Jet Propulsion Laboratory (Sander et al., 2006) (hereinafter "JPL06") and the International Union of Pure and Applied Chemistry (Atkinson et al., 2006) (hereinafter "IUPAC06"). We implemented the Fast-JX radiative transfer code for calculation of photolysis rate constants (Wild et al., 2000; Bian and Prather, 2002), including updates to absorption cross-sections and quantum yields from JPL06. Total ozone columns used as input to Fast-JX are from daily measurements by the Ozone Monitoring Instrument (OMI) satellite instrument with 1°×1° resolution (ftp://toms.gsfc.nasa.gov/pub/omi/data/ozone/Y2008/). The range of ozone columns during ARCTAS was 380∼430 Dobson Units. Fast-JX includes a background climatology of zonal mean profiles of monthly ozone and temperature (Wild et al., 2000). Surface albedo used in Fast-JX is from the Total Ozone Mapping Spectrometer (TOMS) satellite monthly climatology with 1°×1.25° resolution (Herman and Celarier, 1997).

A major topic of this paper will be the role of HO_2 uptake by aerosol. GEOS-Chem simulates aerosol mass concentrations for several aerosol components: sulfate-nitrate-ammonium (Park et al., 2004), size-resolved mineral dust (Fairlie et al., 2007), fine and coarse sea salt (Alexander et al., 2005), and black carbon and organic carbon (Park et al., 2003). For each aerosol component, the model calculates an effective area-weighted radius (r_e) dependent on local relative humidity (RH) (Köpke et al., 1997; Chin et al., 2002).

Gas uptake by each aerosol component is then represented following R. V. Martin et al. (2003) by a first-order uptake rate constant k:

$$k = -\left(\frac{r_e}{D_g} + \frac{4}{v\gamma}\right)^{-1} A \quad (1)$$

where v is the mean molecular speed of the gas, D_g is the gas-phase molecular diffusion coefficient, γ is the reactive uptake coefficient for the gas, and A is the aerosol surface area per unit volume of air calculated from the mass concentration and effective radius of that aerosol component. D_g is calculated as a function of molecular weight, temperature, and air density. We ignore heterogeneous chemistry of HO_x radicals in clouds because the aircraft sampled almost exclusively in clear sky and the regional effects of clouds on the HO_x budget are limited by the small mass fraction of the atmosphere actually occupied by cloud (Jacob, 2000).

The standard model includes aerosol uptake of NO_2, NO_3, and N_2O_5 (Jacob, 2000; Evans and Jacob, 2005) and aqueous-phase reaction of H_2O_2 with SO_2 in cloud (Park et al., 2004). Earlier versions also included aerosol uptake of HO_2 (R. V. Martin et al., 2003), but this was removed in v7-04-06 (and hence in the v8-01-04 version that we used) on the basis of laboratory data indicating low γ values in the absence of transition metal catalysts (Thornton and Abbatt, 2005; Sauvage et al., 2007). More recent standard versions of GEOS-Chem (v8-02-01 and beyond), developed after this work was initiated, include HO_2 uptake following Thornton et al. (2008). As we will show below, the ARCTAS observations suggest an important role for aerosol uptake of HO_2 under the cold, low-light, and relatively aerosol-rich conditions of Arctic spring.

Anthropogenic emissions in GEOS-Chem are as described in van Donkelaar et al. (2008). A prominent feature of ARCTAS flights was the influence of Siberian fire plumes (Warneke et al., 2009). Daily biomass burning emissions for 2008 with $1^\circ \times 1^\circ$ resolution are specified from the Fire Locating and Monitoring of Burning Emissions (FLAMBE) emission inventory (Reid et al., 2009) constrained by GOES and MODIS fire count data. Further details on model emissions are given by Fisher et al. (2010a).

The model wet deposition scheme is described by Liu et al. (2001). It includes wet scavenging in convective updrafts as well as grid-resolved first-order rainout and washout. Of particular interest here is the representation of peroxide and HCHO scavenging. For warm clouds ($T > 268$ K), H_2O_2, CH_3OOH, and HCHO are scavenged by liquid water based on their Henry's law constants. For mixed clouds ($248 < T < 268$ K), precipitation is assumed to take place by riming of liquid cloud droplets with retention efficiencies $R_{H_2O_2} = 0.05$, R_{CH_3OOH}=0.02, and R_{HCHO}=0.02 (Mari et al., 2000). In cold clouds ($T < 248$ K), scavenging of H_2O_2 takes place by co-condensation on ice surfaces while scavenging of CH_3OOH and HCHO are considered negligible (Mari et al., 2000).

Dry deposition is calculated using a standard resistance-in-series scheme (Wesely, 1989) applied to the local surface. For snow and ice the deposition velocity of H_2O_2 is in the range 0.1–0.3 cm s^{-1}, while dry deposition of CH_3OOH and HCHO are negligible. Snow emission could offset dry deposition for the above species (Frey et al., 2005, 2006) but is not taken into account here as its effect would be confined to the shallow boundary layer. For the same reason we find dry deposition to be unimportant from a tropospheric column perspective.

All comparisons between model and observations use model output sampled along the flight tracks and at the flight time with 15-min time resolution. We exclude all measurements in the stratosphere as diagnosed by an ozone/CO molar ratio greater than 1.25. This excludes 72% of the data above 10 km, 41% of the data at 8–10 km, and 9% of the data at 6–8 km. We also exclude all measurements at latitudes lower than 60° N. In order to assess the effect of GEOS-Chem errors for species driving HO_x chemistry (such as ozone, CO, NO), we compare results to those of a gas-phase photochemical box model (Olson et al., 2004) constrained locally by the ARCTAS observations (Olson et al., 2010). Similar comparisons between GEOS-Chem and this box model have been conducted in previous aircraft campaigns (Olson et al., 2004; Hudman et al., 2007; Zhang et al., 2008).

Previous comparisons of the GEOS-Chem HO_x simulation to aircraft LIF measurements from the same Pennsylvania State University group have been reported for the NASA INTEX-A campaign over North America (summer 2004) and the NASA INTEX-B campaign over the North Pacific (spring 2006). Hudman et al. (2007) reported a model overestimate of 30–60% for both OH and HO_2 in INTEX-A, but subsequent recalibration of the measurements resolved the discrepancy (Ren et al., 2008). Zhang et al. (2008) found no model bias for HO_2 in INTEX-B but a 27% high bias for OH. The global mean (mass-weighted) tropospheric OH concentration in our ARCTAS simulation is 10.3×10^5 molecules cm^{-3}, consistent with the multimodel annual mean of $11.1 \pm 1.7 \times 10^5$ molecules cm^{-3} from the intercomparison by Shindell et al. (2006).

3 Median distributions

Figure 1 presents median vertical profiles of OH, HO_2, H_2O_2, CH_3OOH, NO, NO_2, HCHO and HNO_4 concentrations for 1 km vertical bins during ARCTAS. We compare here the observed profiles (black) to results from the standard GEOS-Chem simulation not including HO_2 uptake by aerosols (dashed green line). Also shown in Fig. 1 are model simulations including HO_2 uptake, which will be discussed in Sect. 4. Most data were collected under sunlit conditions, between 08:00 and 18:00 local time. Stratospheric data were excluded as described in Sect. 2. Mean observed temperature and relative humidity (RH) relative to liquid water are 256 K

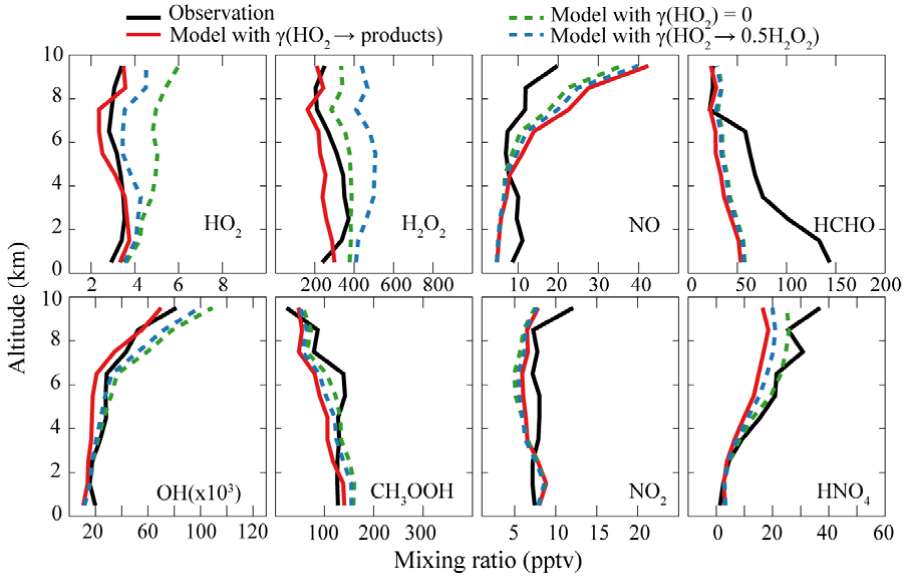

Fig. 1. Median vertical profiles of HO_2, OH, H_2O_2, CH_3OOH, NO, NO_2, HCHO, and HNO_4 concentrations during ARCTAS in the North American Arctic (1–21 April 2008). Observations from the DC-8 aircraft (black lines) are compared to three GEOS-Chem model simulations: 1) without HO_2 uptake by aerosol (green dashed line), referred to in the text as "standard GEOS-Chem"; 2) with HO_2 uptake yielding H_2O_2 (blue dashed line); 3) with HO_2 uptake not yielding H_2O_2 (solid red line). All concentrations are in unit of pptv except OH (ppqv). Most data were collected under sunlit conditions, between 08:00 and 18:00 local time. Stratospheric data were excluded as described in the text.

and 73% at 0–3 km, 243 K and 48% at 3–6 km, and 226 K and 48% above 6 km, consistent with the model. Mean observed $J(O^1D)$ and $J(NO_2)$ agree with the model within 25% and 10% respectively.

Observed concentrations of OH are relatively low (20 ppqv=5×10^5 molecules cm^{-3} in surface air) reflecting the low water vapor, low solar elevation, and thick ozone columns characteristic of Arctic spring. The model reproduces the vertical gradient of the observed OH and its concentrations at 1–6 km within 15%, but is too low by 40% in the surface layer (0–1 km) and too high by 40% in upper troposphere (>6 km). The discrepancy in the surface layer may be due to the effect of halogen chemistry, while the discrepancy in the upper troposphere can be explained by HO_2 aerosol uptake as described in Sect. 4.

Observed concentrations of HO_2, H_2O_2, and CH_3OOH show little altitude dependence, consistent with TOPSE (Wang et al., 2003) but in contrast to measurements in the tropics and northern mid-latitudes that show decreases with altitude driven by water vapor (Cohan et al., 1999; O'Sullivan et al., 1999; Hudman et al., 2007; Snow et al., 2007; Zhang et al., 2008). The model reproduces this lack of vertical structure in the Arctic spring observations and attributes it in part to a strong vertical gradient of UV radiation (low solar angles, thick ozone columns) compensating for the water vapor gradient, and in part to influx of peroxides from northern mid-latitudes in the upper troposphere.

The standard simulation overestimates HO_2 by up to a factor of 2, with the largest discrepancy in the upper troposphere. H_2O_2 is also underestimated. This cannot be explained by model error in the species driving HO_x production, as Olson et al. (2010) find a similar discrepancy for HO_2 in their box model results constrained by ARCTAS observations. They further show that the discrepancy cannot be resolved by adjusting observed concentrations within their measurement uncertainties. A similar overestimate of HO_2 and H_2O_2 was previously found in TOPSE when comparing box model calculations to observations (Cantrell et al., 2003b; Wang et al., 2003). We propose below that aerosol uptake of HO_2 leading to a terminal sink for HO_y could explain the discrepancy between model and observations.

Median observed NO_x concentrations increase from 16 pptv in the boundary layer to 21 pptv in the upper troposphere (>6 km). The model is consistent within the measurement uncertainty (15%±10 pptv), increasing from 13 pptv in the boundary layer to 28 pptv in the upper troposphere. April observations from TOPSE at 60–80° N showed a mean NO concentration of 6 pptv (Wang et al., 2003), consistent with the ARCTAS observations and with the model. A sensitivity model simulation with no fuel emissions shows a 40% mean decrease of NO_x along the ARCTAS flight tracks, while a sensitivity simulation with no biomass burning emissions shows only a 5% decrease. We conclude that a large fraction of the NO_x in ARCTAS was anthropogenic.

Peroxynitric acid (HNO_4) is an important reservoir for HO_x in the upper troposphere at northern mid-latitudes (Jaeglé et al., 2001). ARCTAS observations are below the detection limit in the lower troposphere due to thermal dissociation but increase to 30 pptv in the upper troposphere. The model reproduces the observed concentrations and vertical gradient within the measurement uncertainty.

Observed HCHO decreases with altitude, from 140 pptv near the surface to 25 pptv in the upper troposphere. TOPSE observations by a similar absorption spectrometer using a tunable lead-salt diode laser averaged 95 pptv below 0.2 km and 60 pptv at 6–8 km (Fried et al., 2003). A different laser source, based on tunable difference frequency generation (DFG), was employed in ARCTAS (Weibring et al., 2007; Richter et al., 2009). Model values decrease from 50 pptv near the surface to 30 pptv in the upper troposphere. The discrepancy below 3 km is outside the stated precision of the measurements (26 pptv). Olson et al. (2010) find a similar discrepancy in their box model simulation of the ARCTAS data, and Fried et al. (2003) also reported a low model bias relative to the TOPSE data. Previous GEOS-Chem evaluation with observed HCHO vertical profiles at northern mid-latitudes by the same investigator show no such discrepancy (Palmer et al., 2003; Millet et al., 2006). Halogen radical chemistry and snow emissions of HCHO could provide additional HCHO sources in the boundary layer. However, this does not explain discrepancies between 0.5 and 3 km given the short lifetime of HCHO (hours). Inlet artifact can be ruled out because zero air was added to the inlet every minute as instrument background signal. Singh et al. (2000) suggested a heterogeneous conversion from CH_3OH to HCHO, but we find no correlation between these two species below 4 km (R<0.01). As pointed out in Sect. 5, the source of HO_x and HO_y implied by the observed HCHO appears inconsistent with independent calculations of HO_x and HO_y sinks from the ARCTAS observations, leading to an even higher overestimate of HO_2.

4 HO_2 uptake by aerosols

4.1 Parameterization of uptake

A prominent feature of the comparison between model and observations in Fig. 1 is the overestimate of HO_2. Such a discrepancy between model and observations has been reported in a number of previous studies and tentatively attributed to HO_2 uptake by aerosols (Cantrell et al., 1996a, b; Plummer et al., 1996; Jaeglé et al., 2000; Kanaya et al., 2000; Sommariva et al., 2004; de Reus et al., 2005; Sommariva et al., 2006). This uptake has been reported in a number of laboratory studies but rates and mechanism are uncertain (Jacob, 2000). It could be particularly important in the Arctic because of the low temperature, relatively high aerosol, and slow photochemical cycling.

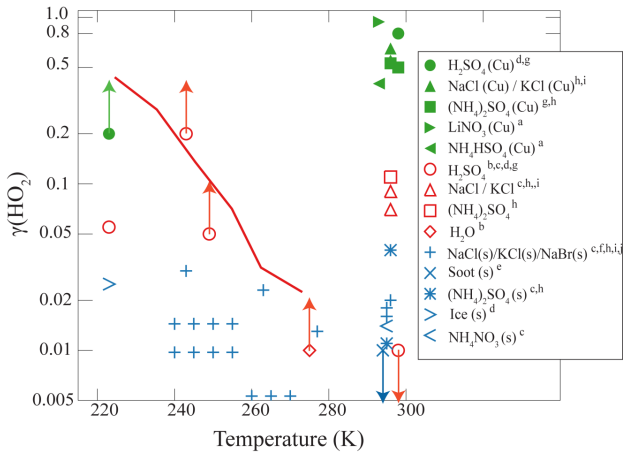

Fig. 2. Laboratory data reported in the literature for the reactive uptake coefficient $\gamma(HO_2)$ by different surfaces as a function of temperature. Vertical arrows indicate "greater than" or "less than". Open symbols indicate aqueous surfaces, closed symbols indicate copper-doped aqueous surfaces, and other symbols indicate solid surfaces (noted as (s) in the legend). The solid red line is the median value of $\gamma(HO_2)$ computed in GEOS-Chem along the ARCTAS flight tracks using the Thornton et al. (2008) parameterization. Literature references are given by footnotes in legend: **(a)** Mozurkewich et al. (1987); **(b)** Hanson et al. (1992); **(c)** Gershenzon et al. (1995); **(d)** Cooper and Abbatt (1996); **(e)** Saathoff et al. (2001); **(f)** Remorov et al. (2002); **(g)** Thornton and Abbatt (2005); **(h)** Taketani et al. (2008); **(i)** Taketani et al. (2009), **(j)** Loukhovitskaya et al. (2009).

Figure 2 summarizes literature data of the HO_2 reactive uptake coefficient $\gamma(HO_2)$ or different surface types. $\gamma(HO_2)$ is defined as the fraction of HO_2 collisions with the aerosol surface resulting in reaction. Consistently high values ($\gamma(HO_2)$>0.2) are observed for Cu-doped aqueous surfaces. Soluble copper is known to drive rapid catalytic conversion of HO_2 to H_2O_2 by redox chemistry (Jacob, 2000). Other values for aqueous surfaces at room temperature are also relatively high ($\gamma(HO_2)$ in the range 0.07–0.2) except for concentrated H_2SO_4 ($\gamma(HO_2)$<0.01). However, $\gamma(HO_2)$or concentrated H_2SO_4 increases rapidly with decreasing temperature and exceeds 0.2 at 240 K. Reactive uptake coefficients in general increase with decreasing temperature, reflecting negative temperature dependences of both the mass accommodation coefficient α on the surface and the solubility constant (Kolb et al., 1995). Solid surfaces do not take up HO_2 significantly. To our knowledge no data are available for $\gamma(HO_2)$ on organic surfaces.

A high reactive uptake probability ($\gamma(HO_2)$>0.1) is needed for aerosol uptake to compete in the atmosphere with other chemical sinks for HO_x. This requires that the aerosol be aqueous, which cannot be directly determined from the ARCTAS observations. Aerosol measurements aboard the P-3 show that non-refractory submicron

particles contributed more than 90% of total surface area (McNaughton et al., 2010). High-resolution Aerosol Mass Spectrometer (AMS; DeCarlo et al., 2006) measurements aboard the DC-8 show an average mass composition for non-refractory submicron particles of 58% sulfate, 32% organic aerosol, 6% ammonium, 3% nitrate, and 0.7% chloride (Cubison et al., 2008). An ammonium vs. sulfate molar plot for the AMS data (Fig. 3) shows dominance of the acidic NH_4HSO_4 form, although in some cases the aerosol was close to sulfuric acid while in other cases it was fully neutralized as $(NH_4)_2SO_4$. Because of metastability of the aqueous phase, both NH_4HSO_4 and $(NH_4)_2SO_4$ are expected to remain aqueous over the range of RH values experienced in ARCTAS (Onasch et al., 1999; S. T. Martin et al., 2003; Colberg et al., 2004). Sulfuric acid is aqueous under all conditions. In addition, Parsons et al. (2004) found that the crystallization RH of ammonium sulfate aerosol decreases as the organic fraction increases. We assume therefore that the aerosol surface area in ARCTAS was mainly contributed by aqueous particles.

To investigate the role of HO_2 uptake by aerosol in our ARCTAS simulations, we included the $\gamma(HO_2)$ parameterization of Thornton et al. (2008) as implemented in the most recent standard versions of GEOS-Chem (v8-02-01 and beyond). This parameterization describes HO_2 uptake by aqueous aerosol as driven by acid-base dissociation followed by the $HO_2(aq)+O_2^-$ reaction at an assumed pH 5, producing H_2O_2 that then volatilizes to the gas phase. It is clearly inconsistent with the prevailing acidic conditions observed in ARCTAS (Fig. 3), and is also theoretically incorrect since it describes HO_2 uptake as a second-order process while the $\gamma(HO_2)$ parameterization intrinsically describes a first-order process. Nevertheless, as shown in Fig. 2 (solid line), it yields values of $\gamma(HO_2)$, that are consistent with those measured in the laboratory for acidic surfaces, ranging from less than 0.05 near the surface to 0.4 in the upper troposphere. Its temperature dependence (mainly driven by the Henry's law constant for HO_2) is consistent with the laboratory data for concentrated H_2SO_4 (Fig. 2). We adopt the Thornton et al. (2008) scheme here to compute $\gamma(HO_2)$ for want of anything better and because it fits the overall laboratory data for acid aerosols.

The fate of HO_2 in aerosol phase is generally assumed to involve conversion to H_2O_2 followed by H_2O_2 volatilization (Jacob, 2000). However, this would exacerbate the overestimate of H_2O_2 in ARCTAS (Fig. 1). One possible solution would be protonation of H_2O_2 to $HOOH_2^+$, a very strong oxidant (Oiestad et al., 2001), which would rapidly react and convert to H_2O. However, this requires normal acidity (pH<0) to be effective (Bach and Su, 1994). Such a mechanism could conceivably take place in concentrated H_2SO_4 aerosols, but not in the less acidic aerosol that prevailed under ARCTAS conditions (Fig. 3).

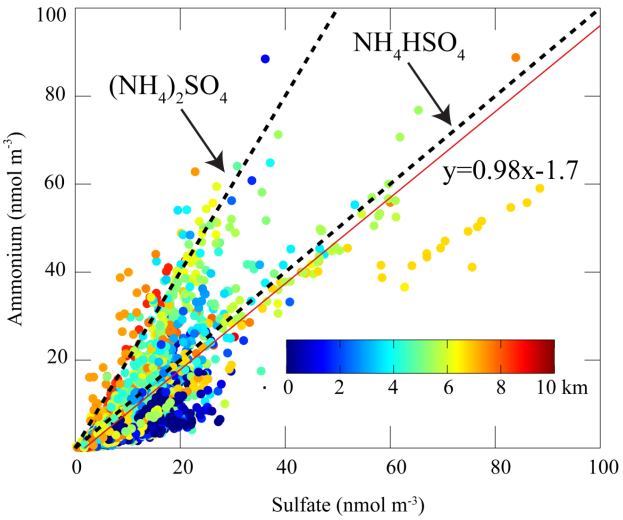

Fig. 3. Scatterplot of observed ammonium vs. sulfate submicron aerosol concentrations measured aboard the DC-8 aircraft during ARCTAS-A (April 2008). The observed points are colored by altitude (km). The data from the first two flights (1 and 4 April) are excluded due to low quality of the ammonium data. In red is the linear least squares regression line for all altitudes.

Another possible solution is that HO_2 uptake may not produce H_2O_2. Cooper and Abbatt (1996) proposed that HO_2 could react with HSO_4^-, forming the peroxymonosulfate radical SO_5^-:

$$HO_2 + HSO_4^- \rightarrow SO_5^- + H_2O \quad \text{(R6)}$$

The possible atmospheric chemistry of the SO_5^- radical is discussed by Jacob (1986), who proposed that the dominant sinks would be the exothermic reactions with O_2^-, $HCOO^-$, and HSO_3^-, all producing the peroxide HSO_5^- (peroxymonosulfate). Peroxymonosulfate is the first dissociated form of Caro's acid (H_2SO_5, highly hygroscopic solid at room temperature, melting point 45 °C), which has first and second acid dissociation constants (pK_a) of 0.4 and 9.1 (Elias et al., 1994). As a peroxide, HSO_5^- is a member of the HO_y family and so its formation does not necessarily represent a terminal sink of HO_x. However, Jacob (1986) suggested that the subsequent fate of HSO_5^- in acidic solution might follow Reactions (R7) or (R8), either of which provides a terminal sink for HO_y by conversion to water:

$$HSO_5^- + OH \rightarrow SO_5^- + H_2O \quad \text{(R7)}$$

$$HSO_5^- + HSO_3^- + H^+ \rightarrow 2SO_4^{2-} + 2H^+ \quad \text{(R8)}$$

Another possible mechanism for uptake of HO_2 by sulfate aerosols might involve the formation of an HO_2 complex. Miller and Francisco (2001) found from quantum chemical calculations that a stable HO_2-H_2SO_4 complex can be formed in the gas as well as in the aerosol phase. HSO_4^- has

similar potential for bonding with HO_2 molecules (C. Miller, personal communication, 2009). The fate of these complexes is unknown. They must not decompose to the original reactants if they are to represent an actual HO_x or HO_y sink. One possibility would be conversion to SO_5^- by Reaction (R6), with subsequent chemistry forming HSO_5^- and eventually returning water as described above.

4.2 Application to the ARCTAS simulation

Figure 1 shows the results of two simulations, one with HO_2 aerosol uptake producing H_2O_2 ($\gamma(HO_2 \rightarrow 0.5H_2O_2)$, dashed blue line), and the other with HO_2 aerosol uptake leading to a permanent HO_y sink as postulated above ($\gamma(HO_2 \rightarrow$products), red line). Mean aerosol surface area in the model corrected by hygroscopic growth factors (R. V. Martin et al., 2003) is 26 $\mu m^2\,cm^{-3}$ at 0–3 km, 33 $\mu m^2\,cm^{-3}$ at 3–6 km and 19 $\mu m^2\,cm^{-3}$ above 6 km. The model agrees with the measurements of aerosol surface area aboard the P-3 within a factor of 2. The simulation with $\gamma(HO_2 \rightarrow 0.5H_2O_2)$ worsens the overestimate of H_2O_2, as aerosol uptake now competes with other HO_x sinks such as $OH+HO_2$ and $CH_3O_2+HO_2$ that do not produce H_2O_2. The correction to HO_2 is also insufficient in the upper troposphere as H_2O_2 can be recycled to HO_x by photolysis. The simulation with $\gamma(HO_2 \rightarrow$products) provides a much better fit to the observations for both HO_2 and H_2O_2, though H_2O_2 is now too low in the middle troposphere. It also improves the fit for OH, while not significantly affecting the fits for the other species. OH concentrations decrease by up to 36% in the upper troposphere.

Figure 4 shows scatterplots of simulated vs. observed OH, HO_2, H_2O_2, and CH_3OOH concentrations for the model simulation with $\gamma(HO_2 \rightarrow$products) and the ensemble of tropospheric observations in ARCTAS. The slopes of the reduced-major-axis regression lines are within the measurement accuracy for all species. Correlation coefficients for OH (R=0.61) and HO_2 (R=0.81) are only slightly improved from the gas-phase-only simulation (R=0.58 and R=0.78 respectively). Correlations are weak for H_2O_2 (R=0.45) and CH_3OOH (R=0.50), which might reflect the narrow dynamic range. The HO_2 variability is mostly correlated with solar zenith angle in both the observations and the model (R=−0.8 in both cases), with additional significant correlations with water vapor (R=0.3 observed, R=0.4 model) and temperature (R=0.3 observed, R=0.4 model) above 4 km. The correlation of HO_2 concentrations with temperature offers some supporting evidence for a sink from aerosol uptake. The DC-8 did not include measurements of aerosol surface area that we could correlate to HO_2 concentrations, but in the model we find that temperature is a much stronger driver of $\gamma(HO_2)$ variability than aerosol surface area. No correlation is found between HO_2 and NO_x concentrations in either the model or the observations.

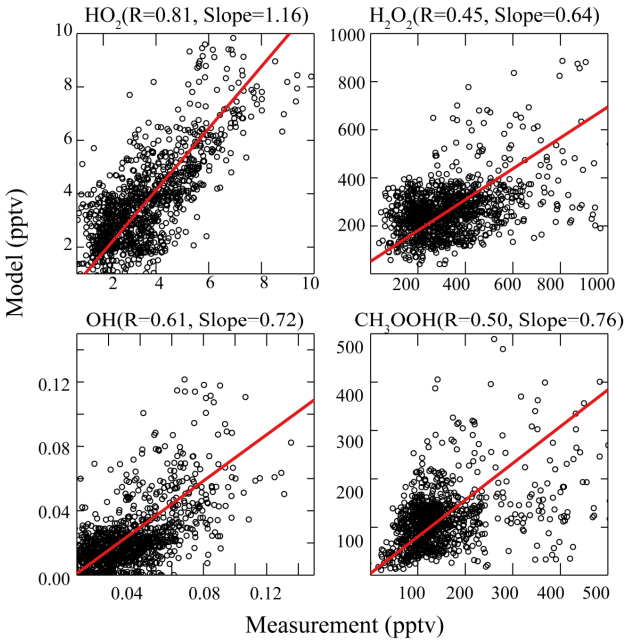

Fig. 4. Scatterplots of simulated vs. observed HO_2, OH, H_2O_2, and CH_3OOH concentrations, for the model simulation with $\gamma(HO_2 \rightarrow$products) and the ensemble of tropospheric observations during ARCTAS (April 2008). The red solid line is the reduced major axis regression line. Panel titles give the correlation coefficients and regression slopes.

5 Budget of HO_x radicals in Arctic spring

We now proceed to quantify the budgets of HO_x and HO_y in Arctic spring as constrained by the ARCTAS observations and derived from the model. We use for that purpose the model including terminal loss of HO_y from reactive uptake of HO_2 by aerosols as described in Sect. 4.1. Even though the process is uncertain, it represents our best hypothesis for explaining the HO_x and peroxide observations in ARCTAS.

Figure 5 shows the median vertical profiles of major HO_x source and sink terms computed from the observed ARCTAS concentrations, gas-phase reaction rate constants from JPL06 and IUPAC06, and $\gamma(HO_2 \rightarrow$products) from Thornton et al. (2008). Formation of organic nitrates is negligible in the HO_x and HO_y budgets, at least in the model, and is not included in Fig. 5. The CH_3O_2 concentration is assumed to be 30% of that of HO_2 on the basis of the model HO_2/CH_3O_2 ratio. HO_2 aerosol uptake is computed using local model values for γ and aerosol surface area. O (^{1}D)+H_2O and HCHO photolysis are the major HO_x sources below 4 km. Above that altitude the photolysis of H_2O_2 becomes dominant, a remarkable feature that has not been reported to our knowledge anywhere else in the troposphere. It reflects the low OH concentrations in Arctic spring and therefore the dominance of photolysis as a H_2O_2 sink rather than reaction with OH (Fig. 5).

The HO_2+HO_2 reaction is the principal HO_x sink in the lower troposphere but HO_2 uptake by aerosol becomes dominant above 5 km. HO_x sinks from CH_3O_2+HO_2 and OH+HO_2 are relatively small. The NO_x-based HO_x sinks including HO_2+NO_2, OH+HNO_4, and OH+NO_2 are negligibly small because of the low NO_x concentrations, so that gross ozone production is NO_x-limited throughout the troposphere (Jaeglé et al., 2001). In contrast, previous aircraft campaigns at northern mid-latitudes (SONEX, INTEX-A) found that the NO_x-based reactions dominated the HO_x sink in the upper troposphere, implying NO_x-neutral or NO_x-saturated conditions for ozone production (Jaeglé et al., 2000; Ren et al., 2008). The observed NO_x concentrations in the upper troposphere in these campaigns (medians of 93 pptv in SONEX, 440 pptv in INTEX-A) are much higher than in ARCTAS (21 pptv), reflecting major sources at northern mid-latitudes from convective injection of pollution and lightning (Jaeglé et al., 1998; Allen et al., 2000; Hudman et al., 2007).

We see from Fig. 5 that HO_2 uptake by aerosols is crucial for balancing the HO_x sources with the HO_x sinks independently computed from observations, at least in the upper troposphere. There the main gas-phase sinks (HO_2+HO_2, CH_3O_2+HO_2, OH+HO_2) can balance only 20% of the HO_x source. With HO_2 uptake by aerosol included in the budget, the total HO_x sinks balance 50% of the HO_x sources in the lower troposphere (0–3 km) and 70% in the upper troposphere (>6 km). The imbalance in the lower troposphere reflects the high observed HCHO concentrations (Fig. 1), for which we have no explanation. The aerosol sink is ineffective in the lower troposphere because of the relatively high temperatures (average T=258 K at 0–2 km, resulting in $\gamma(HO_2)$=0.06). Loss of HO_2 by uptake by aerosol has a first-order dependence on HO_x concentration, whereas the gas-phase sinks have a quadratic dependence. However, we find that the total HO_x source $P(HO_x)$ computed from Fig. 5 is strongly correlated in the upper troposphere with both observed [HO_2] (R=0.87) and [HO_2]^2 (R=0.85), so that it does not test the sink mechanism.

Figure 5 also shows the median vertical profiles of instantaneous HO_y source and sink terms, again computed from the measurements. The main HO_y sources are O(^{1}D)+H_2O and HCHO photolysis. The main sinks are HO_2 uptake by aerosol and the gas-phase OH+CH_3OOH reaction. OH+H_2O_2 is relatively unimportant due to its much slower rate constant (1.8×10^{-12} cm^3 molecules^{-1} s^{-1}, no temperature dependence) compared to OH+CH_3OOH (3.8×10^{-12} exp(200/T) cm^3 molecules^{-1} s^{-1}) as given by JPL06. Such a dominance of the gas-phase HO_y sink by the OH+CH_3OOH reaction has not been reported before to our knowledge, except in deep convective outflow where H_2O_2 has been scavenged but not CH_3OOH (Cohan et al., 1999). We attribute it to the low concentrations of NO_x in Arctic spring, suppressing the NO_x-based HO_x sinks (see discussion above) and promoting CH_3OOH formation.

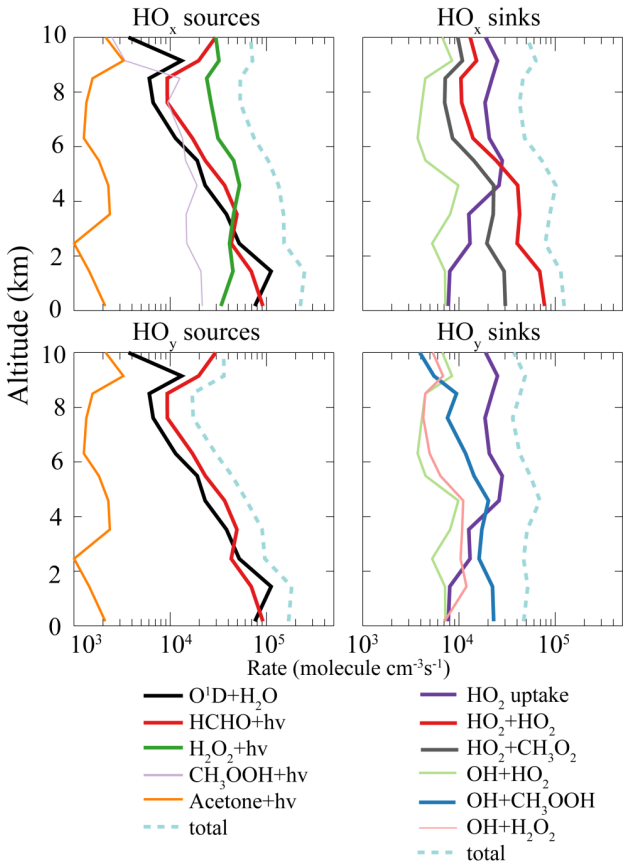

Fig. 5. Median vertical profiles of major HO_x and HO_y sources and sinks computed from observed tropospheric concentrations in ARCTAS (April 2008). Values are instantaneous rates. Only important processes are shown. Gas-phase rate constants are from JPL06 and IUPAC06. HO_2 uptake by aerosol is computed with a reaction probability $\gamma(HO_2 \rightarrow \text{products})$ from Thornton et al. (2008). Stratospheric data are excluded as described in the text.

Figure 5 shows an imbalance between HO_y chemical sources and sinks that reverses sign with altitude. The HO_y sink balances 30% of the source below 3 km, 92% at 3–6 km, and 170% above 6 km. The HO_y lifetime is 2–6 d, sufficiently long that additional terms may be relevant in the HO_y budget including long-range transport, wet and dry deposition, and aqueous-phase oxidation of SO_2 by H_2O_2 in clouds. To consider the effect of these terms, we conducted a HO_y budget analysis in the GEOS-Chem model averaged over the 60–90° N circumpolar Arctic cap. Results are shown in Fig. 6. The budget in the model is balanced by mass conservation; the excess of HO_y sources over HO_y sinks in the tropospheric column reflects accumulation of peroxides over the course of April.

We see from Fig. 6 that influx of peroxides from northern mid-latitudes in the model accounts for 50% of the total HO_y source above 6 km and 20% at 3–6 km. This explains the chemical imbalance in the HO_y budget constrained by

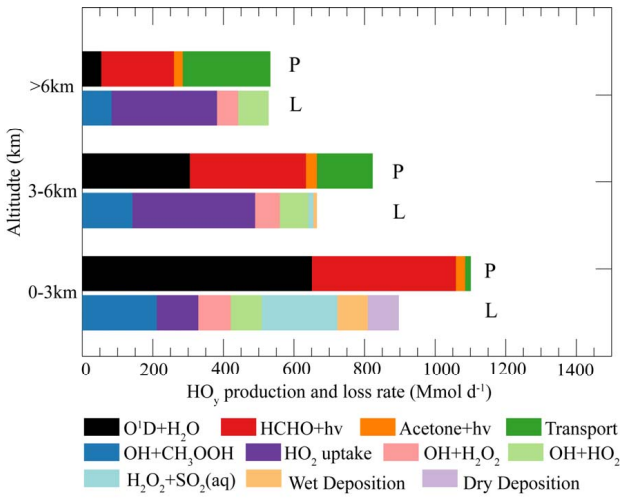

Fig. 6. Circumpolar GEOS-Chem model budget of HO_y for the Arctic tropospheric column (60–90° N) during ARCTAS (1–21 April 2008). Mean production rates (P) and loss rates (L) are shown for three altitude bands. The transport term describes exchange with northern mid-latitudes south of 60° N.

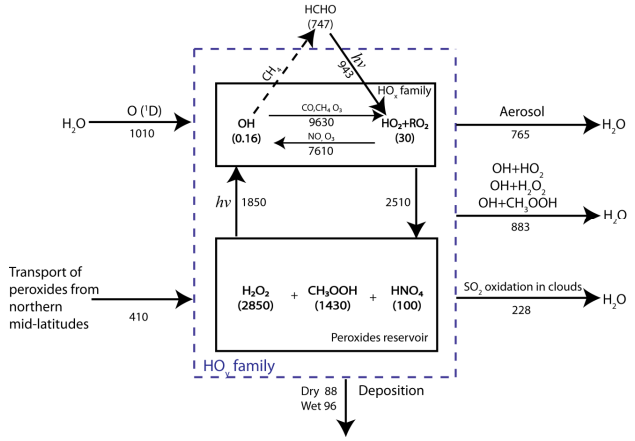

Fig. 7. Schematic diagram of HO_x-HO_y chemistry in Arctic spring as constructed from the GEOS-Chem model simulation of the ARCTAS observations. Values are tropospheric column averages for April 2008 over the Arctic cap (60–90° N). Masses of chemicals within the domain (in parentheses) are in units of Mmol and rates are in units of Mmol d^{-1}. The dashed line for HCHO production indicates that it is not a HO_y sink.

the ARCTAS observations (Fig. 5). Considering the dominant role of H_2O_2 photolysis as a source of HO_x above 5 km (Fig. 5), this implies a significant contribution of northern mid-latitudes to the HO_x budget of the Arctic free troposphere. Below 3 km, we find in the model that cloud chemistry and deposition of H_2O_2 together account for 40% of the HO_y sink. This helps but is insufficient to correct the chemical imbalance in the HO_y budget constrained by the observations. As in the case of the HO_x budget, the residual imbalance reflects the high observed HCHO.

Figure 7 gives a summary diagram of the HO_x and HO_y cycling as represented by our model for Arctic spring. Primary sources include the O (^{1}D)+H_2O reaction within the region (70%) and transport of peroxides from northern mid-latitudes (30%). Photolysis of HCHO produced from oxidation of methane by OH is a major amplifying source of HO_y, of comparable magnitude to the primary source from O(^{1}D)+H_2O. HO_2 aerosol uptake accounts for 35% of the HO_y sink. Cycling within the HO_x family (between OH and peroxy radicals) is relatively efficient (chain length=3.4) given the low NO_x concentrations. This is because formation of peroxides to terminate the chain is slow as a result of the low HO_x concentrations.

6 Implications

The ARCTAS observations show a large missing sink of HO_x and HO_y in Arctic spring relative to current understanding. If our hypothesis that this reflects a fast terminal loss of HO_2 to aerosols is correct, then it implies a significant sensitivity of the oxidizing power of the Arctic atmosphere to aerosol perturbations. A measure of this effect is provided by the difference in Fig. 1 between our standard simulation (solid red line) and the gas-only simulation (dashed green line). In the absence of aerosols, OH and HO_2 concentrations would increase on average respectively by 32% and 31% in the tropospheric column, the largest effects being in the upper troposphere where uptake by aerosol is particularly efficient (low temperatures). Biomass burning from Siberian wildfires was a major aerosol source to the Arctic in ARCTAS (Warneke et al., 2009), and this aerosol was mainly organic for which we have no information on HO_2 uptake. We find in a sensitivity simulation with no biomass burning that OH and HO_2 concentrations would increase respectively by 10% and 9% in the tropospheric column.

Uptake of HO_2 by aerosol is expected to be particularly efficient as a sink for HO_x in Arctic spring because of the combination of cold temperatures, relatively high aerosol concentrations, and weak UV radiation. On a global scale, however, the OH budget is mainly determined by the tropics and mid-latitudes summer where aerosol uptake would be less important. We find in our model that the global mean tropospheric OH concentration decreases by 3% when we include uptake of HO_2 by aerosols as described here.

Laboratory data show a wide range for the reactive uptake coefficient $\gamma(HO_2)$, as summarized in Fig. 2. Increasing confidence in the role of aerosols for HO_x uptake will require better characterization of $\gamma(HO_2)$ and its temperature dependence, including in particular for organic aerosol (aqueous and non-aqueous). For the aerosol loadings in Arctic spring, a value $\gamma(HO_2)>0.1$ averaged over the aerosol surface area is necessary for uptake to be important.

The HO_2 chemistry in the aerosol phase is another critical issue to resolve. The only product study to our knowledge is that of Loukhovitskaya et al. (2009), who found H_2O_2 to be the main product for solid NaBr surfaces. It is conventionally assumed that uptake by aqueous aerosols would also produce H_2O_2 from the $HO_2(aq)+O_2^-$ self-reaction (Thornton et al., 2008) or from catalytic cycles involving transition metal ions (Graedel et al., 1986). We find that an HO_2 uptake mechanism producing H_2O_2 would overestimate the observed H_2O_2 concentrations in ARCTAS, though the mechanism not producing H_2O_2 underestimates the observed H_2O_2 in middle troposphere, suggesting perhaps a contribution from both mechanisms. A mechanism not producing H_2O_2 might involve reaction of HO_2 with acid sulfate to produce peroxymonosulfate (HSO_5^-). Mechanisms and products for HO_2 uptake by different aerosol types need to be studied in the laboratory. Considering that HO_2 uptake by aerosols has opposite effects on H_2O_2 depending on whether or not H_2O_2 is produced as a result of uptake, changes in aerosol types (biomass burning vs. fossil fuel) or aerosol acidity (sulfuric acid vs. ammonium) could have large effects on H_2O_2. This may be relevant to explaining the complex long-term trend of H_2O_2 observed in Greenland ice cores (Möller, 1999).

Acknowledgements. The authors would like to thank Scot T. Martin, Hongyu Liu, Charles E. Miller, Richard A. Ferrare, Karl D. Froyd and Daniel M. Murphy for helpful discussions. We also would like to thank Yuhang Wang for providing the TOPSE dataset, Huisheng Bian for providing Fast-JX updates and Dirk Richter for contributing to the HCHO measurement. J. Mao also thanks David M. Shelow and the NASA DC-8 crew for their generous help with making HO_x measurements on the aircraft. This work was supported by the NASA Tropospheric Chemistry Program.

Edited by: P. Monks

References

Alexander, B., Park, R. J., Jacob, D. J., Li, Q. B., Yantosca, R. M., Savarino, J., Lee, C. C. W., and Thiemens, M. H.: Sulfate formation in sea-salt aerosols: Constraints from oxygen isotopes, J. Geophys. Res.-Atmos., 110, D10307, doi:10.1029/2004jd005659, 2005.

Allen, D., Pickering, K., Stenchikov, G., Thompson, A., and Kondo, Y.: A three-dimensional total odd nitrogen (NOy) simulation during SONEX using a stretched-grid chemical transport model, J. Geophys. Res.-Atmos., 105, 3851–3876, 2000.

Atkinson, R., Baulch, D. L., Cox, R. A., Crowley, J. N., Hampson, R. F., Hynes, R. G., Jenkin, M. E., Rossi, M. J., Troe, J., and IUPAC Subcommittee: Evaluated kinetic and photochemical data for atmospheric chemistry: Volume II – gas phase reactions of organic species, Atmos. Chem. Phys., 6, 3625–4055, doi:10.5194/acp-6-3625-2006, 2006.

Bach, R. D. and Su, M. D.: The transition-state for the hydroxylation of saturated-hydrocarbons with hydroperoxonium ion, J. Am. Chem. Soc., 116, 10103–10109, 1994.

Bey, I., Jacob, D. J., Yantosca, R. M., Logan, J. A., Field, B. D., Fiore, A. M., Li, Q. B., Liu, H. G. Y., Mickley, L. J., and Schultz, M. G.: Global modeling of tropospheric chemistry with assimilated meteorology: Model description and evaluation, J. Geophys. Res.-Atmos., 106, 23073–23095, 2001.

Bian, H. S. and Prather, M. J.: Fast-J2: Accurate simulation of stratospheric photolysis in global chemical models, J. Atmos. Chem., 41, 281–296, 2002.

Bloss, W. J., Lee, J. D., Johnson, G. P., Sommariva, R., Heard, D. E., Saiz-Lopez, A., Plane, J. M. C., McFiggans, G., Coe, H., Flynn, M., Williams, P., Rickard, A. R., and Fleming, Z. L.: Impact of halogen monoxide chemistry upon boundary layer OH and HO_2 concentrations at a coastal site, Geophys. Res. Lett., 32(4), L06814, doi:10.1029/2004GL022084, 2005.

Browne E., Wooldrige, P., and Cohen, R.: ΣPNs, $CH_3O_2NO_2$ and NO_x Observations: Comparisons to TOPSE ΣPNs/O_3, in preparation, 2010.

Cantrell, C. A., Shetter, R. E., Gilpin, T. M., and Calvert, J. G.: Peroxy radicals measured during Mauna Loa observatory photochemistry experiment 2: The data and first analysis, J. Geophys. Res.-Atmos., 101, 14643–14652, 1996a.

Cantrell, C. A., Shetter, R. E., Gilpin, T. M., Calvert, J. G., Eisele, F. L., and Tanner, D. J.: Peroxy radical concentrations measured and calculated from trace gas measurements in the Mauna Loa observatory photochemistry experiment 2, J. Geophys. Res.-Atmos., 101, 14653–14664, 1996b.

Cantrell, C. A., Edwards, G. D., Stephens, S., Mauldin, L., Kosciuch, E., Zondlo, M., and Eisele, F.: Peroxy radical observations using chemical ionization mass spectrometry during topse, J. Geophys. Res.-Atmos., 108(D6), 8371, doi:10.1029/2002jd002715, 2003a.

Cantrell, C. A., Mauldin, L., Zondlo, M., Eisele, F., Kosciuch, E., Shetter, R., Lefer, B., Hall, S., Campos, T., Ridley, B., Walega, J., Fried, A., Wert, B., Flocke, F., Weinheimer, A., Hannigan, J., Coffey, M., Atlas, E., Stephens, S., Heikes, B., Snow, J., Blake, D., Blake, N., Katzenstein, A., Lopez, J., Browell, E. V., Dibb, J., Scheuer, E., Seid, G., and Talbot, R.: Steady state free radical budgets and ozone photochemistry during TOPSE, J. Geophys. Res.-Atmos., 108(D4), 8361, doi:10.1029/2002jd002198, 2003b.

Chen, G., Davis, D., Crawford, J., Hutterli, L. M., Huey, L. G., Slusher, D., Mauldin, L., Eisele, F., Tanner, D., Dibb, J., Buhr, M., McConnell, J., Lefer, B., Shetter, R., Blake, D., Song, C. H., Lombardi, K., and Arnoldy, J.: A reassessment of HO_x south pole chemistry based on observations recorded during ISCAT 2000, Atmos. Environ., 38, 5451–5461, doi:10.1016/j.atmosenv.2003.07.018, 2004.

Chen, G., Olson, J., and Crawford, J. H.: Intercomparison during ARCTAS, in preparation, 2010.

Chin, M., Ginoux, P., Kinne, S., Torres, O., Holben, B. N., Duncan, B. N., Martin, R. V., Logan, J. A., Higurashi, A., and Nakajima, T.: Tropospheric aerosol optical thickness from the gocart model and comparisons with satellite and sun photometer measurements, J. Atmos. Sci., 59, 461–483, 2002.

Cohan, D. S., Schultz, M. G., Jacob, D. J., Heikes, B. G., and Blake, D. R.: Convective injection and photochemical decay of peroxides in the tropical upper troposphere: Methyl iodide as a tracer of marine convection, J. Geophys. Res.-Atmos., 104, 5717–5724, 1999.

Colberg, C. A., Krieger, U. K., and Peter, T.: Morphological investigations of single levitated $H_2SO_4/NH_3/H_2O$ aerosol particles during deliquescence/efflorescence experiments, J. Phys. Chem. A, 108, 2700–2709, doi:10.1021/jp037628r, 2004.

Cooper, P. L. and Abbatt, J. P. D.: Heterogeneous interactions of OH and HO_2 radicals with surfaces characteristic of atmospheric particulate matter, J. Phys. Chem., 100, 2249–2254, 1996.

Cubison, M. J., Sueper, D., Dunlea, E. J., and Jimenez, J. L.: Submicron aerosol composition during the arctas campaign: Arctic haze, biomass burning, and california pollution, EOS Transaction AGU, 89, Fall Meet. Suppl. A11A-0081, 2008.

de Reus, M., Fischer, H., Sander, R., Gros, V., Kormann, R., Salisbury, G., Van Dingenen, R., Williams, J., Zöllner, M., and Lelieveld, J.: Observations and model calculations of trace gas scavenging in a dense Saharan dust plume during MINATROC, Atmos. Chem. Phys., 5, 1787–1803, doi:10.5194/acp-5-1787-2005, 2005.

DeCarlo, P. F., Kimmel, J. R., Trimborn, A., Northway, M. J., Jayne, J. T., Aiken, A. C., Gonin, M., Fuhrer, K., Horvath, T., Docherty, K. S., Worsnop, D. R., and Jimenez, J. L.: Field-deployable, high-resolution, time-of-flight aerosol mass spectrometer, Anal. Chem., 78, 8281–8289, doi:10.1021/ac061249n, 2006.

Dibb, J., Scheuer E., Jordan C., Emmons L., and Anderson B.: Source regions and transport pathways for aerosol in the north American Arctic in April, in preparation, 2010.

Elias, H., Gotz, U., and Wannowius, K. J.: Kinetics and mechanism of the oxidation of sulfur(IV) by peroxomonosulfuric acid anion, Atmos. Environ., 28, 439–448, 1994.

Evans, M. J., Jacob, D. J., Atlas, E., Cantrell, C. A., Eisele, F., Flocke, F., Fried, A., Mauldin, R. L., Ridley, B. A., Wert, B., Talbot, R., Blake, D., Heikes, B., Snow, J., Walega, J., Weinheimer, A. J., and Dibb, J.: Coupled evolution of BrO_x-ClO_x-HO_x-NO_x chemistry during bromine-catalyzed ozone depletion events in the arctic boundary layer, J. Geophys. Res.-Atmos., 108(D4), 8368, doi:10.1029/2002jd002732, 2003.

Evans, M. J. and Jacob, D. J.: Impact of new laboratory studies of N_2O_5 hydrolysis on global model budgets of tropospheric nitrogen oxides, ozone, and OH, Geophys. Res. Lett., 32, L09813, doi:10.1029/2005gl022469, 2005.

Fairlie, T. D., Jacob, D. J., and Park, R. J.: The impact of transpacific transport of mineral dust in the united states, Atmos. Environ., 41, 1251–1266, doi:10.1016/j.atmosenv.2006.09.048, 2007.

Fisher, J. A., Jacob, D. J., Purdy, M. T., Kopacz, M., Le Sager, P., Carouge, C., Holmes, C. D., Yantosca, R. M., Batchelor, R. L., Strong, K., Diskin, G. S., Fuelberg, H. E., Holloway, J. S., Hyer, E. J., McMillan, W. W., Warner, J., Streets, D. G., Zhang, Q., Wang, Y., and Wu, S.: Source attribution and interannual variability of Arctic pollution in spring constrained by aircraft (ARCTAS, ARCPAC) and satellite (AIRS) observations of carbon monoxide, Atmos. Chem. Phys., 10, 977–996, doi:10.5194/acp-10-977-2010, 2010a.

Fisher J. A., Jacob, D. J., Dibb, J. E., Scheuer E., Jimenez, J. L., and Cubison, M.: Sources and acidity of sulfate-nitrate-ammonium aerosol in the Arctic in spring, in preparation, 2010b.

Frey, M. M., Stewart, R. W., McConnell, J. R., and Bales, R. C.: Atmospheric hydroperoxides in West Antarctica: Links to stratospheric ozone and atmospheric oxidation capacity, J. Geophys. Res.-Atmos., 110, D23301, doi:10.1029/2005jd006110, 2005.

Frey, M. M., Bales, R. C., and McConnell, J. R.: Climate sensitivity of the century-scale hydrogen peroxide (H_2O_2) record preserved in 23 ice cores from West Antarctica, J. Geophys. Res.-Atmos., 111, D21301, doi:10.1029/2005jd006816, 2006.

Fried, A., Wang, Y. H., Cantrell, C., Wert, B., Walega, J., Ridley, B., Atlas, E., Shetter, R., Lefer, B., Coffey, M. T., Hannigan, J., Blake, D., Blake, N., Meinardi, S., Talbot, B., Dibb, J., Scheuer, E., Wingenter, O., Snow, J., Heikes, B., and Ehhalt, D.: Tunable diode laser measurements of formaldehyde during the TOPSE 2000 study: Distributions, trends, and model comparisons, J. Geophys. Res.-Atmos., 108(D4), 8365, doi:10.1029/2002jd002208, 2003.

Fried A., Richter D., Weibring P., Apel, E. C., Gorham, K. A., Walega J., Blake, D. R., Blake, N. J., Orlando, J. J., Weinheimer, A., Knapp, D. J., Huey, L. G., and Meinardi, S.: Airborne formaldehyde and VOC measurements during select Arctic boundary layer runs in the 2008 ARCTAS study and estimates of Halogen atom mixing ratios, in preparation, 2010.

Gershenzon, Y. M., Grigorieva, V. M., Ivanov, A. V., and Remorov, R. G.: O_3 and OH sensitivity to heterogeneous sinks of HO_x and CH_3O_2 on aerosol particles, Faraday Discuss., 100, 83–100, 1995.

Graedel, T. E., Mandich, M. L., and Weschler, C. J.: Kinetic-model studies of atmospheric droplet chemistry: 2. Homogeneous transition-metal chemistry in raindrops, J. Geophys. Res.-Atmos., 91, 5205–5221, 1986.

Hanson, D. R., Burkholder, J. B., Howard, C. J., and Ravishankara, A. R.: Measurement of OH and HO_2 radical uptake coefficients on water and sulfuric-acid surfaces, J. Phys. Chem., 96, 4979–4985, 1992.

Herman, J. R. and Celarier, E. A.: Earth surface reflectivity climatology at 340-380 nm from toms data, J. Geophys. Res.-Atmos., 102, 28003–28011, 1997.

Honrath, R. E., Peterson, M. C., Guo, S., Dibb, J. E., Shepson, P. B., and Campbell, B.: Evidence of NO_x production within or upon ice particles in the greenland snowpack, Geophys. Res. Lett., 26, 695–698, 1999.

Hudman, R. C., Jacob, D. J., Turquety, S., Leibensperger, E. M., Murray, L. T., Wu, S., Gilliland, A. B., Avery, M., Bertram, T. H., Brune, W., Cohen, R. C., Dibb, J. E., Flocke, F. M., Fried, A., Holloway, J., Neuman, J. A., Orville, R., Perring, A., Ren, X., Sachse, G. W., Singh, H. B., Swanson, A., and Wooldridge, P. J.: Surface and lightning sources of nitrogen oxides over the united states: Magnitudes, chemical evolution, and outflow, J. Geophys. Res.-Atmos., 112, D12s05, doi:10.1029/2006JD007912, 2007.

Hutterli, M. A., McConnell, J. R., Stewart, R. W., Jacobi, H. W., and Bales, R. C.: Impact of temperature-driven cycling of hydrogen peroxide (H_2O_2) between air and snow on the planetary boundary layer, J. Geophys. Res.-Atmos., 106, 15395–15404, 2001.

Hutterli, M. A., McConnell, J. R., Chen, G., Bales, R. C., Davis, D. D., and Lenschow, D. H.: Formaldehyde and hydrogen peroxide in air, snow and interstitial air at South Pole, Atmos. Environ., 38, 5439–5450, doi:10.1016/j.atmosenv.2004.06.003, 2004.

Jacob, D. J.: Chemistry of OH in remote clouds and its role in the production of formic-acid and peroxymonosulfate, J. Geophys. Res.-Atmos., 91, 9807–9826, 1986.

Jacob, D. J.: Heterogeneous chemistry and tropospheric ozone, Atmos. Environ., 34, 2131–2159, 2000.

Jacob, D. J., Crawford, J. H., Maring, H., Clarke, A. D., Dibb, J. E., Emmons, L. K., Ferrare, R. A., Hostetler, C. A., Russell, P. B.,

Singh, H. B., Thompson, A. M., Shaw, G. E., McCauley, E., Pederson, J. R., and Fisher, J. A.: The Arctic Research of the Composition of the Troposphere from Aircraft and Satellites (ARCTAS) mission: design, execution, and first results, Atmos. Chem. Phys., 10, 5191–5212, doi:10.5194/acp-10-5191-2010, 2010.

Jacobi, H. W., Frey, M. M., Hutterli, M. A., Bales, R. C., Schrems, O., Cullen, N. J., Steffen, K., and Koehler, C.: Measurements of hydrogen peroxide and formaldehyde exchange between the atmosphere and surface snow at Summit, Greenland, Atmos. Environ., 36, 2619–2628, 2002.

Jaeglé, L., Jacob, D. J., Wennberg, P. O., Spivakovsky, C. M., Hanisco, T. F., Lanzendorf, E. J., Hintsa, E. J., Fahey, D. W., Keim, E. R., Proffitt, M. H., Atlas, E. L., Flocke, F., Schauffler, S., McElroy, C. T., Midwinter, C., Pfister, L., and Wilson, J. C.: Observed OH and HO_2 in the upper troposphere suggest a major source from convective injection of peroxides, Geophys. Res. Lett., 24, 3181–3184, 1997.

Jaeglé, L., Jacob, D. J., Wang, Y., Weinheimer, A. J., Ridley, B. A., Campos, T. L., Sachse, G. W., and Hagen, D. E.: Sources and chemistry of NO_x in the upper troposphere over the united states, Geophys. Res. Lett., 25, 1705–1708, 1998.

Jaeglé, L., Jacob, D. J., Brune, W. H., Faloona, I., Tan, D., Heikes, B. G., Kondo, Y., Sachse, G. W., Anderson, B., Gregory, G. L., Singh, H. B., Pueschel, R., Ferry, G., Blake, D. R., and Shetter, R. E.: Photochemistry of HO_x in the upper troposphere at northern midlatitudes, J. Geophys. Res.-Atmos., 105, 3877–3892, 2000.

Jaeglé, L., Jacob, D. J., Brune, W. H., and Wennberg, P. O.: Chemistry of HO_x radicals in the upper troposphere, Atmos. Environ., 35, 469–489, 2001.

Kahl, J. D.: Characteristics of the low-level temperature inversion along the Alaskan Arctic coast, Int. J. Climatol., 10, 537–548, 1990.

Kanaya, Y., Sadanaga, Y., Matsumoto, J., Sharma, U. K., Hirokawa, J., Kajii, Y., and Akimoto, H.: Daytime HO_2 concentrations at Oki Island, Japan, in summer 1998: Comparison between measurement and theory, J. Geophys. Res.-Atmos., 105, 24205–24222, 2000.

Kolb, C. E., Worsnop, D. R., Zahniser, M. S., Davidovits, P., Keyser, L. F., Leu, M.-T., Molina, M. J., Hanson, D. R., and Ravishankara, A. R.: Laboratory studies of atmospheric heterogeneous chemistry, in: Progress and problems in atmospheric chemistry, edited by: Baker, J., Advanced series in physical chemistry, 3, 771–875, 1995.

Köpke, P., Hess, M., Schult, I., and Shettle, E. P.: Global aerosol data set, report, Max-Planck Inst. für Meteorol., Hamburg, Germany, 1997.

Liao, J., Huey, L. G., Scheuer, E., and Dibb, J. E.: Characterization of soluble bromide measurements during ARCTAS, in preparation, 2010.

Liang, J. Y. and Jacob, D. J.: Effect of aqueous phase cloud chemistry on tropospheric ozone, J. Geophys. Res.-Atmos., 102, 5993–6001, 1997.

Liu, H. Y., Jacob, D. J., Bey, I., and Yantosca, R. M.: Constraints from Pb-210 and Be-7 on wet deposition and transport in a global three-dimensional chemical tracer model driven by assimilated meteorological fields, J. Geophys. Res.-Atmos., 106, 12109–12128, 2001.

Loukhovitskaya, E., Bedjanian, Y., Morozov, I., and Le Bras, G.: Laboratory study of the interaction of HO_2 radicals with the NaCl, NaBr, $MgCl_26H_2O$ and sea salt surfaces, Phys. Chem. Chem. Phys., 11, 7896–7905, doi:10.1039/b906300e, 2009.

Mari, C., Jacob, D. J., and Bechtold, P.: Transport and scavenging of soluble gases in a deep convective cloud, J. Geophys. Res.-Atmos., 105, 22255–22267, 2000.

Martin, R. V., Jacob, D. J., Yantosca, R. M., Chin, M., and Ginoux, P.: Global and regional decreases in tropospheric oxidants from photochemical effects of aerosols, J. Geophys. Res.-Atmos., 108(D3), 4097, doi:10.1029/2002jd002622, 2003.

Martin, S. T., Schlenker, J. C., Malinowski, A., Hung, H. M., and Rudich, Y.: Crystallization of atmospheric sulfate-nitrate-ammonium particles, Geophys. Res. Lett., 30(21), 2102, doi:10.1029/2003gl017930, 2003.

McNaughton, C. S., Clarke, A.D. , Freitag, S., Kapustin, V. N., Kondo, Y., Moteki, N., Sahu, L. K., Takegawa, N., Schwarz, J. P., Spackman, J. R., Diskin, G. S., Sachse, G. W., Podolske, J. R., Holloway, J., Wisthaler, A., Mikoviny, T., De Gouw, J. A., Warneke, C., Jimenez, J. L., Cubison, M., Howell, S., Middlebrook, A. M., Bahreini, R., Anderson, B., Winstead, E. L., Thornhill, K. L., Lack, D. A., Cozic, J., and Brock, C. A.: Absorbing aerosol in the troposphere of the Western Arctic during the 2008 ARCTAS/ARCPAC airborne field campaigns, in preparation, 2010.

Miller, C. E. and Francisco, J. S.: The formation of a surprisingly stable HO_2-H_2SO_4 complex, J. Am. Chem. Soc., 123, 10387–10388, 2001.

Millet, D. B., Jacob, D. J., Turquety, S., Hudman, R. C., Wu, S. L., Fried, A., Walega, J., Heikes, B. G., Blake, D. R., Singh, H. B., Anderson, B. E., and Clarke, A. D.: Formaldehyde distribution over North America: Implications for satellite retrievals of formaldehyde columns and isoprene emission, J. Geophys. Res.-Atmos., 111, D24s02, doi:10.1029/2005jd006853, 2006.

Möller, D.: Explanation for the recent dramatic increase of H_2O_2 concentrations found in Greenland ice cores, Atmos. Environ., 33, 2435–2437, 1999.

Mozurkewich, M., McMurry, P. H., Gupta, A., and Calvert, J. G.: Mass accommodation coefficient for HO_2 radicals on aqueous particles, J. Geophys. Res.-Atmos., 92, 4163–4170, 1987.

Müller, J. F. and Brasseur, G.: Sources of upper tropospheric HO_x: A three-dimensional study, J. Geophys. Res.-Atmos., 104, 1705–1715, 1999.

Neuman, J. A., Nowak, J. B., Huey, L. G., Burkholder, J. B., Dibb, J. E., Holloway, J. S., Liao, J., Peischl, J., Roberts, J. M., Ryerson, T. B., Scheuer, E., Stark, H., Stickel, R. E., Tanner, D. J., and Weinheimer, A.: Bromine measurements in ozone depleted air over the Arctic Ocean, Atmos. Chem. Phys. Discuss., 10, 3827–3860, doi:10.5194/acpd-10-3827-2010, 2010.

O'Sullivan, D. W., Heikes, B. G., Lee, M., Chang, W., Gregory, G. L., Blake, D. R., and Sachse, G. W.: Distribution of hydrogen peroxide and methylhydroperoxide over the pacific and south atlantic oceans, J. Geophys. Res.-Atmos., 104, 5635–5646, 1999.

Oiestad, A. M. L., Petersen, A. C., Bakken, V., Vedde, J., and Uggerud, E.: The oxidative power of protonated hydrogen peroxide, Angew. Chem.-Int. Edit., 40, 1305–1309, 2001.

Olson, J. R., Crawford, J. H., Chen, G., Brune, W. H., Ren, X., Wennberg, P. O., Fried, A. and Mao, J.: Photochemical Analysis of ARCTAS Observations, in preparation, 2010.

Olson, J. R., Crawford, J. H., Chen, G., Fried, A., Evans, M. J.,

Jordan, C. E., Sandholm, S. T., Davis, D. D., Anderson, B. E., Avery, M. A., Barrick, J. D., Blake, D. R., Brune, W. H., Eisele, F. L., Flocke, F., Harder, H., Jacob, D. J., Kondo, Y., Lefer, B. L., Martinez, M., Mauldin, R. L., Sachse, G. W., Shetter, R. E., Singh, H. B., Talbot, R. W., and Tan, D.: Testing fast photochemical theory during TRACE-P based on measurements of OH, HO_2, and CH_2O, J. Geophys. Res.-Atmos., 109(16), D15s10, doi:10.1029/2003jd004278, 2004.

Onasch, T. B., Siefert, R. L., Brooks, S. D., Prenni, A. J., Murray, B., Wilson, M. A., and Tolbert, M. A.: Infrared spectroscopic study of the deliquescence and efflorescence of ammonium sulfate aerosol as a function of temperature, J. Geophys. Res.-Atmos., 104, 21317–21326, 1999.

Palmer, P. I., Jacob, D. J., Fiore, A. M., Martin, R. V., Chance, K., and Kurosu, T. P.: Mapping isoprene emissions over north america using formaldehyde column observations from space, J. Geophys. Res.-Atmos., 108(D6), 4180, doi:10.1029/2002jd002153, 2003.

Park, R. J., Jacob, D. J., Chin, M., and Martin, R. V.: Sources of carbonaceous aerosols over the united states and implications for natural visibility, J. Geophys. Res.-Atmos., 108, 4355, doi:10.1029/2002jd003190, 2003.

Park, R. J., Jacob, D. J., Field, B. D., Yantosca, R. M., and Chin, M.: Natural and transboundary pollution influences on sulfate-nitrate-ammonium aerosols in the united states: Implications for policy, J. Geophys. Res.-Atmos., 109, D15204, doi:10.1029/2003jd004473, 2004.

Park, R. J., Jacob, D. J., Kumar, N., and Yantosca, R. M.: Regional visibility statistics in the united states: Natural and transboundary pollution influences, and implications for the regional haze rule, Atmos. Environ., 40, 5405–5423, doi:10.1016/j.atmosenv.2006.04.059, 2006.

Parsons, M. T., Knopf, D. A., and Bertram, A. K.: Deliquescence and crystallization of ammonium sulfate particles internally mixed with water-soluble organic compounds, J. Phys. Chem. A, 108, 11600–11608, doi:10.1021/jp0462862, 2004.

Plummer, D. A., McConnell, J. C., Shepson, P. B., Hastie, D. R., and Niki, H.: Modeling of ozone formation at a rural site in southern ontario, Atmos. Environ., 30, 2195–2217, 1996.

Prather, M. J. and Jacob, D. J.: A persistent imbalance in HO_x and NO_x photochemistry of the upper troposphere driven by deep tropical convection, Geophys. Res. Lett., 24, 3189–3192, 1997.

Quinn, P. K., Bates, T. S., Baum, E., Doubleday, N., Fiore, A. M., Flanner, M., Fridlind, A., Garrett, T. J., Koch, D., Menon, S., Shindell, D., Stohl, A., and Warren, S. G.: Short-lived pollutants in the Arctic: their climate impact and possible mitigation strategies, Atmos. Chem. Phys., 8, 1723–1735, doi:10.5194/acp-8-1723-2008, 2008.

Reid, J. S., Hyer, E. J., Prins, E. M., Westphal, D. L., Zhang, J. L., Wang, J., Christopher, S. A., Curtis, C. A., Schmidt, C. C., Eleuterio, D. P., Richardson, K. A., and Hoffman, J. P.: Global monitoring and forecasting of biomass-burning smoke: Description of and lessons from the Fire Locating And Modeling of Burning Emissions (FLAMBE) program, IEEE J. Sel. Topics Appl. Earth Observations Remote Sens., 2, 144–162, doi:10.1109/jstars.2009.2027443, 2009.

Remorov, R. G., Gershenzon, Y. M., Molina, L. T., and Molina, M. J.: Kinetics and mechanism of HO_2 uptake on solid NaCl, J. Phys. Chem. A, 106, 4558–4565, doi:10.1021/jp013179o, 2002.

Ren, X. R., Olson, J. R., Crawford, J. H., Brune, W. H., Mao, J. Q., Long, R. B., Chen, Z., Chen, G., Avery, M. A., Sachse, G. W., Barrick, J. D., Diskin, G. S., Huey, L. G., Fried, A., Cohen, R. C., Heikes, B., Wennberg, P. O., Singh, H. B., Blake, D. R., and Shetter, R. E.: Hox chemistry during intex-a 2004: Observation, model calculation, and comparison with previous studies, J. Geophys. Res.-Atmos., 113, D05310,10.1029/2007jd009166, 2008.

Richter, D., Fried, A., and Weibring, P.: Difference frequency generation laser based spectrometers, Laser Photo. Rev., 3, 343–354, doi:10.1002/lpor.200810048, 2009.

Ridley, B., Walega, J., Montzka, D., Grahek, F., Atlas, E., Flocke, F., Stroud, V., Deary, J., Gallant, A., Boudries, H., Bottenheim, J., Anlauf, K., Worthy, D., Sumner, A. L., Splawn, B., and Shepson, P.: Is the arctic surface layer a source and sink of NO_x in winter/spring?, J. Atmos. Chem., 36, 1–22, 2000.

Saathoff, H., Naumann, K. H., Riemer, N., Kamm, S., Mohler, O., Schurath, U., Vogel, H., and Vogel, B.: The loss of NO_2, HNO_3, NO_3/N_2O_5, and $HO_2/HOONO_2$ on soot aerosol: A chamber and modeling study, Geophys. Res. Lett., 28, 1957–1960, 2001.

Salawitch, R. J., Canty, T. P., Kurosu, T. P., Chance, K., Liang, Q., Pawson, S., Liu, X., Huey, L. G., Liao, J., Stickel, R. E., Tanner, D., Dibb, J. E., Weinheimer, A. J., Flocke, F. M., Knapp, D. J., Montzka, D. D., Neuman, J., Simpson, W. R., Donohoue, D., Carlson, D., Blake, D. R., Kinnison, D. E., Tilmes, S., Pan, L., Pierce, R., Hendrick, F., Kreher, K., Wang, Y., Choi, S., and Atlas, E. L.: Airborne, Ground-based, and Satellite Measurements of BrO during ARCTAS and ARCPAC, in preparation, 2010.

Sander, S. P., Friedl, R. R., Ravishankara, A. R., Golden, D. M., and Kurylo, M. J.: Chemical kinetics and photochemical data for use in atmospheric studies, Evaluation Number 15, 2006.

Sauvage, B., Martin, R. V., van Donkelaar, A., Liu, X., Chance, K., Jaegl, L., Palmer, P. I., Wu, S., and Fu, T.-M.: Remote sensed and in situ constraints on processes affecting tropical tropospheric ozone, Atmos. Chem. Phys., 7, 815–838, doi:10.5194/acp-7-815-2007, 2007.

Scheuer, E., Talbot, R. W., Dibb, J. E., Seid, G. K., DeBell, L., and Lefer, B.: Seasonal distributions of fine aerosol sulfate in the north american arctic basin during TOPSE, J. Geophys. Res.-Atmos., 108(D4), 8370, doi:10.1029/2001jd001364, 2003.

Shindell, D. T., Faluvegi, G., Stevenson, D. S., Krol, M. C., Emmons, L. K., Lamarque, J. F., Petron, G., Dentener, F. J., Ellingsen, K., Schultz, M. G., Wild, O., Amann, M., Atherton, C. S., Bergmann, D. J., Bey, I., Butler, T., Cofala, J., Collins, W. J., Derwent, R. G., Doherty, R. M., Drevet, J., Eskes, H. J., Fiore, A. M., Gauss, M., Hauglustaine, D. A., Horowitz, L. W., Isaksen, I. S. A., Lawrence, M. G., Montanaro, V., Muller, J. F., Pitari, G., Prather, M. J., Pyle, J. A., Rast, S., Rodriguez, J. M., Sanderson, M. G., Savage, N. H., Strahan, S. E., Sudo, K., Szopa, S., Unger, N., van Noije, T. P. C., and Zeng, G.: Multimodel simulations of carbon monoxide: Comparison with observations and projected near-future changes, J. Geophys. Res.-Atmos., 111, D19306, doi:10.1029/2006jd007100, 2006.

Shindell, D. T., Chin, M., Dentener, F., Doherty, R. M., Faluvegi, G., Fiore, A. M., Hess, P., Koch, D. M., MacKenzie, I. A., Sanderson, M. G., Schultz, M. G., Schulz, M., Stevenson, D. S., Teich, H., Textor, C., Wild, O., Bergmann, D. J., Bey, I., Bian, H., Cuvelier, C., Duncan, B. N., Folberth, G., Horowitz, L. W., Jonson, J., Kaminski, J. W., Marmer, E., Park, R., Pringle,

K. J., Schroeder, S., Szopa, S., Takemura, T., Zeng, G., Keating, T. J., and Zuber, A.: A multi-model assessment of pollution transport to the Arctic, Atmos. Chem. Phys., 8, 5353–5372, doi:10.5194/acp-8-5353-2008, 2008.

Simpson, W. R., von Glasow, R., Riedel, K., Anderson, P., Ariya, P., Bottenheim, J., Burrows, J., Carpenter, L. J., Frie, U., Goodsite, M. E., Heard, D., Hutterli, M., Jacobi, H.-W., Kaleschke, L., Neff, B., Plane, J., Platt, U., Richter, A., Roscoe, H., Sander, R., Shepson, P., Sodeau, J., Steffen, A., Wagner, T., and Wolff, E.: Halogens and their role in polar boundary-layer ozone depletion, Atmos. Chem. Phys., 7, 4375–4418, doi:10.5194/acp-7-4375-2007, 2007.

Singh, H., Chen, Y., Tabazadeh, A., Fukui, Y., Bey, I., Yantosca, R., Jacob, D., Arnold, F., Wohlfrom, K., Atlas, E., Flocke, F., Blake, D., Blake, N., Heikes, B., Snow, J., Talbot, R., Gregory, G., Sachse, G., Vay, S., and Kondo, Y.: Distribution and fate of selected oxygenated organic species in the troposphere and lower stratosphere over the Atlantic, J. Geophys. Res.-Atmos., 105, 3795–3805, 2000.

Snow, J. A., Heikes, B. G., Merrill, J. T., Wimmers, A. J., Moody, J. L., and Cantrell, C. A.: Winter-spring evolution and variability of HO_x reservoir species, hydrogen peroxide, and methyl hydroperoxide, in the northern middle to high latitudes, J. Geophys. Res.-Atmos., 108(D4), 8362, doi:10.1029/2002jd002172, 2003.

Snow, J. A., Heikes, B. G., Shen, H. W., O'Sullivan, D. W., Fried, A., and Walega, J.: Hydrogen peroxide, methyl hydroperoxide, and formaldehyde over North America And The North Atlantic, J. Geophys. Res.-Atmos., 112, D12S07, doi:10.1029/2006jd007746, 2007.

Sommariva, R., Haggerstone, A.-L., Carpenter, L. J., Carslaw, N., Creasey, D. J., Heard, D. E., Lee, J. D., Lewis, A. C., Pilling, M. J., and Zádor, J.: OH and HO_2 chemistry in clean marine air during SOAPEX-2, Atmos. Chem. Phys., 4, 839–856, doi:10.5194/acp-4-839-2004, 2004.

Sommariva, R., Bloss, W. J., Brough, N., Carslaw, N., Flynn, M., Haggerstone, A.-L., Heard, D. E., Hopkins, J. R., Lee, J. D., Lewis, A. C., McFiggans, G., Monks, P. S., Penkett, S. A., Pilling, M. J., Plane, J. M. C., Read, K. A., Saiz-Lopez, A., Rickard, A. R., and Williams, P. I.: OH and HO_2 chemistry during NAMBLEX: roles of oxygenates, halogen oxides and heterogeneous uptake, Atmos. Chem. Phys., 6, 1135–1153, doi:10.5194/acp-6-1135-2006, 2006.

Sumner, A. L. and Shepson, P. B.: Snowpack production of formaldehyde and its effect on the arctic troposphere, Nature, 398, 230–233, 1999.

Sumner, A. L., Shepson, P. B., Grannas, A. M., Bottenheim, J. W., Anlauf, K. G., Worthy, D., Schroeder, W. H., Steffen, A., Domine, F., Perrier, S., and Houdier, S.: Atmospheric chemistry of formaldehyde in the arctic troposphere at polar sunrise, and the influence of the snowpack, Atmos. Environ., 36, 2553–2562, 2002.

Taketani, F., Kanaya, Y., and Akimoto, H.: Kinetics of heterogeneous reactions of HO_2 radical at ambient concentration levels with $(NH_4)_2SO_4$ and NaCl aerosol particles, J. Phys. Chem. A, 112, 2370–2377, doi:10.1021/jp0769936, 2008.

Taketani, F., Kanaya, Y., and Akimoto, H.: Heterogeneous loss of HO_2 by KCl, synthetic sea salt, and natural seawater aerosol particles, Atmos. Environ., 43, 1660–1665, doi:10.1016/j.atmosenv.2008.12.010, 2009.

Thornton, J. and Abbatt, J. P. D.: Measurements of HO_2 uptake to aqueous aerosol: Mass accommodation coefficients and net reactive loss, J. Geophys. Res.-Atmos., 110, D08309, doi:10.1029/2004jd005402, 2005.

Thornton, J. A., Jaeglé, L., and McNeill, V. F.: Assessing known pathways for HO_2 loss in aqueous atmospheric aerosols: Regional and global impacts on tropospheric oxidants, J. Geophys. Res.-Atmos., 113, D05303, doi:10.1029/2007jd009236, 2008.

van Donkelaar, A., Martin, R. V., Leaitch, W. R., Macdonald, A. M., Walker, T. W., Streets, D. G., Zhang, Q., Dunlea, E. J., Jimenez, J. L., Dibb, J. E., Huey, L. G., Weber, R., and Andreae, M. O.: Analysis of aircraft and satellite measurements from the Intercontinental Chemical Transport Experiment (INTEX-B) to quantify long-range transport of East Asian sulfur to Canada, Atmos. Chem. Phys., 8, 2999–3014, doi:10.5194/acp-8-2999-2008, 2008.

Wagner, T., Leue, C., Wenig, M., Pfeilsticker, K., and Platt, U.: Spatial and temporal distribution of enhanced boundary layer BrO concentrations measured by the GOME instrument aboard ERS-2, J. Geophys. Res.-Atmos., 106, 24225–24235, 2001.

Wang, Y. H., Ridley, B., Fried, A., Cantrell, C., Davis, D., Chen, G., Snow, J., Heikes, B., Talbot, R., Dibb, J., Flocke, F., Weinheimer, A., Blake, N., Blake, D., Shetter, R., Lefer, B., Atlas, E., Coffey, M., Walega, J., and Wert, B.: Springtime photochemistry at northern mid and high latitudes, J. Geophys. Res.-Atmos., 108(D4), 8358, doi:10.1029/2002jd002227, 2003.

Wang, Q., Jacob, D. J., Fisher, J. A., Mao, J., Le Sager, P., Leibensperger, E. M., Carouge, C., Kondo, Y., Jimenez, J. L., Cubison, M., Howell, S. G., Freitag, S., Clarke, A. D., McNaughton, C. S., Weber, R., and Apel, E. C. : Sources and Sinks of Carbonaceous Aerosols in the Arctic in Spring, in preparation, 2010.

Warneke, C., Bahreini, R., Brioude, J., Brock, C. A., de Gouw, J. A., Fahey, D. W., Froyd, K. D., Holloway, J. S., Middlebrook, A., Miller, L., Montzka, S., Murphy, D. M., Peischl, J., Ryerson, T. B., Schwarz, J. P., Spackman, J. R., and Veres, P.: Biomass burning in Siberia and Kazakhstan as an important source for haze over the Alaskan Arctic in April 2008, Geophys. Res. Lett., 36, L02813, doi:10.1029/2008gl036194, 2009.

Weibring, P., Richter, D., Walega, J. G., and Fried, A.: First demonstration of a high performance difference frequency spectrometer on airborne platforms, Opt. Exp., 15, 13476–13495, 2007.

Wesely, M. L.: Parameterization of surface resistances to gaseous dry deposition in regional-scale numerical-models, Atmos. Environ., 23, 1293–1304, 1989.

Wild, O., Zhu, X., and Prather, M. J.: Fast-j: Accurate simulation of in- and below-cloud photolysis in tropospheric chemical models, J. Atmos. Chem., 37, 245–282, 2000.

Yang, J., Honrath, R. E., Peterson, M. C., Dibb, J. E., Sumner, A. L., Shepson, P. B., Frey, M., Jacobi, H. W., Swanson, A., and Blake, N.: Impacts of snowpack emissions on deduced levels of OH and peroxy radicals at summit, greenland, Atmos. Environ., 36, 2523–2534, 2002.

Zhang, L., Jacob, D. J., Boersma, K. F., Jaffe, D. A., Olson, J. R., Bowman, K. W., Worden, J. R., Thompson, A. M., Avery, M. A., Cohen, R. C., Dibb, J. E., Flock, F. M., Fuelberg, H. E., Huey, L. G., McMillan, W. W., Singh, H. B., and Weinheimer, A. J.: Transpacific transport of ozone pollution and the effect of recent Asian emission increases on air quality in North Amer-

ica: an integrated analysis using satellite, aircraft, ozonesonde, and surface observations, Atmos. Chem. Phys., 8, 6117–6136, doi:10.5194/acp-8-6117-2008, 2008.

Zhou, X. L., Beine, H. J., Honrath, R. E., Fuentes, J. D., Simpson, W., Shepson, P. B., and Bottenheim, J. W.: Snowpack photochemical production of HONO: A major source of OH in the arctic boundary layer in springtime, Geophys. Res. Lett., 28, 4087–4090, 2001.